NATIONAL AERONAUTICS AND SPACE ADMINISTRATION

Technical Report 32-1606

Sustained Load Crack Growth Design Data for Ti-6Al-4V Titanium Alloy Tanks Containing Hydrazine

(NASA-CR-147976) SUSTAINED LOAD CRACK GROWTH DESIGN DATA FOR Ti-6Al-4V TITANIUM ALLOY TANKS CONTAINING HYDRAZINE (Jet Propulsion Lab.) 24 p HC $3.50 CSCL 13M

N76-31567

Unclas
G3/39 03437

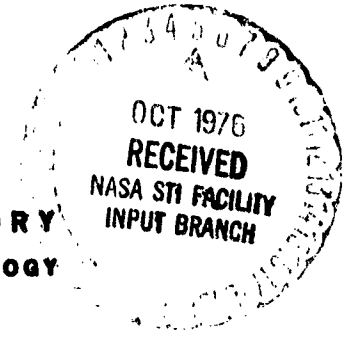

JET PROPULSION LABORATORY
CALIFORNIA INSTITUTE OF TECHNOLOGY
PASADENA, CALIFORNIA

September 15, 1976

NATIONAL AERONAUTICS AND SPACE ADMINISTRATION

Technical Report 32-1606

Sustained Load Crack Growth Design Data for Ti-6Al-4V Titanium Alloy Tanks Containing Hydrazine

J. C. Lewis

Jet Propulsion Laboratory

J. T. Kenny

Martin Marietta Aerospace

JET PROPULSION LABORATORY

CALIFORNIA INSTITUTE OF TECHNOLOGY

PASADENA, CALIFORNIA

September 15, 1976

Preface

The work described in this report was performed by the Applied Mechanics Division of the Jet Propulsion Laboratory.

Acknowledgments

The authors wish to acknowledge the excellent support received from Kenneth Evans and Gordon Thomas for the scanning electron microscopy, John Short for propellant handling, and William Cannon for propellant analyses.

Contents

Tables

Figures

Abstract

Sustained load crack growth data for Ti-6Al-4V titanium alloy in hydrazine per MIL-P-26536 and refined hydrazine are presented. Fracture mechanics data on crack growth thresholds for heat-treated forgings, aged and unaged welds, and aged and unaged heat-affected zones are reported. Fracture mechanics design curves of crack growth threshold stress intensity versus temperature are generated from 40 to 71°C.

Sustained Load Crack Growth Design Data for Ti-6Al-4V Titanium Alloy Tanks Containing Hydrazine

I. Introduction

A. Background

The current fracture control methods used by NASA for aerospace pressure vessels specify a fracture mechanics analysis for each pressure vessel design (Refs. 1–4). This analysis requires that fracture mechanics data on sustained load crack growth (SLCG) be available for the selected pressure vessel material in all operating environments. As a result, the Mariner Jupiter/Saturn 1977 (MJS'77) Project planned to generate sustained load crack growth data for Ti-6Al-4V titanium alloy in hydrazine per MIL-P-26536 at 40°C (105°F) for the MJS'77 Propulsion Subsystem propellant tanks.

B. Low-Cost Systems Approach

Upon learning that the Space Shuttle Orbiter Auxiliary Power Unit (APU) used MIL-P-26536 hydrazine at 66°C (150°F), a proposal was made by the Low-Cost Standardized Spacecraft Equipment Project at JPL to the NASA Low-Cost Systems Office to generate a fracture mechanics design curve for MIL-P-26536 hydrazine in Ti-6Al-4V titanium alloy tanks for the Shuttle APU and for future users of the NASA Standard Hydrazine Attitude Control Thruster/Valve Assembly and the NASA Standard Propellant (Hydrazine) Control Assembly.

By generating 60°C (140°F) and 71°C (160°F) data on the same material heat being used for the 40°C data already funded by the MJS'77 Project, a master design curve for the sustained load crack growth threshold versus temperature could be obtained at little additional cost. Cost studies showed that the first user beyond the MJS'77 Project would totally amortize the additional cost. Consequently, agreement to generate the master design curve (see Fig. 25) was reached with the people at the NASA Johnson Space Center, who are responsible for fracture control of the Space Shuttle.

C. Test Plan

The test matrix for the design data is shown in Table 1. Tests in refined hydrazine at 40°C were conducted to tie the master design curve to the extensive amount of fracture mechanics data for refined hydrazine that had been generated for the Viking Project (Ref. 5). Tests at 40°C on welds and heat-affected zones (HAZ) that had

Table 1. Test matrix for SLCG design data for Ti-6Al-4V titanium alloy in hydrazine[a]

Hydrazine composition	Crack location	Heat-treat condition	Test temperature, °C		
			40	60	71
MIL-P-26536	Forging	Fully aged (STA)	X	X	X
MIL-P-26536	Weld	As welded (unaged)	X	X	X
MIL-P-26536	Weld	Aged after welding	X		
MIL-P-26536	HAZ	As welded (unaged)	X	X	X
MIL-P-26536	HAZ	Aged after welding	X		
Refined	Forging	Fully aged (STA)	X		
Refined	Weld	As welded (unaged)	X		
Refined	HAZ	As welded (unaged)	X		

[a]Exposure time was 24 h for all tests.

been aged after welding were included to make the design curve applicable to those tanks whose design allowed aging after welding. Only unaged welds and HAZ were tested at all three temperatures because most hydrazine tank designs did not permit aging after welding.

II. Materials

A. Forgings

Materials for all specimens were taken from Ti-6Al-4V titanium alloy pressure vessel forgings per MIL-T-9047 from Reactive Metals, Incorporated, Heat No. 301275. All the material for all specimens was solution-treated at 954°C (1750°F) for 1 h, water-quenched to 20°C (68°F) within 5 s, and then aged at 510°C (950°F) for 4 h. A minimum of 0.25 cm was removed from all surfaces after solution-treating and aging. Table 2 gives the chemistry of the forging heat. The mechanical properties of the solution-treated and aged (STA) forgings are given in Table 3. Figure 1 shows a typical microstructure from the forgings. Forging specimen orientation is shown in Fig. 2.

B. Welds and Heat-Affected Zones

Panels of the aged forging material were welded together by Pressure Systems, Incorporated, using the same inert gas welding chamber, semiautomatic gas tungsten arc welding equipment, and procedures as were used to weld the propellant tanks for the two MJS'77 spacecraft to be launched in 1977 to Jupiter and Saturn (Ref. 6). The weld panels were made to the MJS'77 spacecraft propellant tank weld joint configuration (Fig. 3). Two specimens, LCW-25 and MJS-W-He-1, were from a panel made to the Viking Orbiter 1975 (VO'75) spacecraft propellant tank weld joint configuration (Fig. 3). Weld panel orientation is shown in Fig. 2.

After-welding, some of the specimens were aged for 4 h in argon of dew point less than −68°C (−90°F) at 510°C. Most of the specimens were tested with the welds in the "as welded" condition with no aging after welding.

After welding, the weld bead was machined from both sides of the weld, and individual specimens were then sliced from the weld panels. Residual stress analysis showed the weld specimens to be essentially free of residual stress.

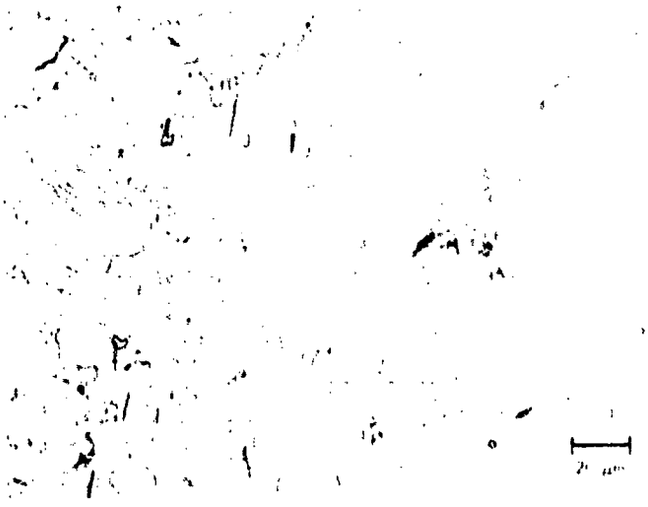

Fig. 1. Typical microstructure of forging material from Reactive Metals, Inc., Heat No. 301275 (Keller's etch)

REPRODUCIBILITY OF THE
ORIGINAL PAGE IS POOR

Table 2. Chemical composition of Ti-6Al-4V titanium alloy forgings from Heat No. RMI 301275

Percent by weight							
C	Fe	N	O	H	Al	V	Ti
0.024	0.14	0.008	0.18	0.0116	6 3	4.3	Balance

Table 3. Mean mechanical properties and sample standard deviations of twelve different pieces of Ti-6Al-4V (STA) titanium alloy from Heat No. RMI 301275

	Ultimate strength, MPa	Yield strength, MPa	Elongation, % in 1.63 cm	Reduction of area, %
$\bar{X}$	1255	1165	8	45
σ	34	34	0.7	3

Table 4 gives the oxygen, nitrogen, and hydrogen content of the unaged weld bead. Typical mechanical properties of the weld are presented in Table 5. Figure 4 shows a typical weld microstructure.

C. Propellants

The basic propellant used in this program was hydrazine (N_2H_4) per MIL-P-26536C, Amendment 1, Monopropellant Grade. Hereinafter, this propellant will be referred to as MIL-Spec hydrazine. Additional tests at 40°C were run in aniline-free, refined hydrazine of very high purity. Actual chemical compositions of the propellants are shown in Table 6.

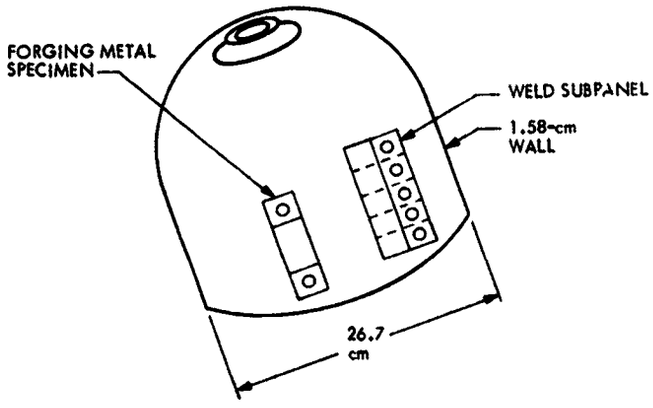

Fig. 3. Weld panel configuration

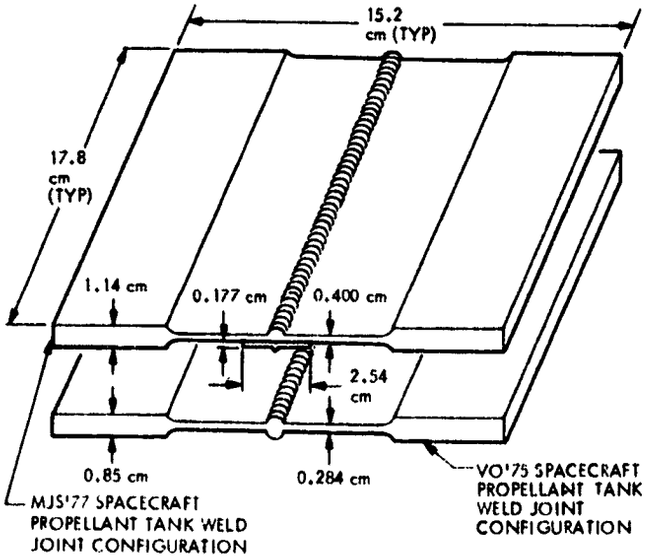

Fig. 2. Specimen location and orientation

Fig. 4. Typical microstructure of MJS'77 spacecraft propellant tank weld joint (Kroll's etch)

Table 4. Oxygen, nitrogen, and hydrogen content of weld bead from specimen MJS-W-1

Percent by weight		
O	N	H
0.14	0.0069	0.0088
0.13		0.0098
		0.0111

Table 5. Mechanical properties of "as welded" weld from Ti-6Al-4V titanium alloy, Heat No. RMI 301275

Ultimate strength, MPa	Yield strength, MPa	Elongation, % in 5.08 cm
1158	1048	3
1158	1041	3
1124	1041	3

Table 6. Propellant compositions

Constituent	Percent by weight	
	Refined hydrazine	MIL-Spec hydrazine
Hydrazine (N_2H_4)	99.0 ± 0.02	98.7 ± 0.02
Water	0.62 ± 0.05	0.61 ± 0.05
Particulate	0.5 ± 0.1	Not determined
Chloride	<0.00005 ± 0.00005	0.0001 ± 0.00005
Aniline	0.0027 ± 0.0005	0.45 ± 0.0005
Iron	0.000074 ± 0.000005	0.00003 ± 0.000005
Nonvolatile residue	0.002 ± 0.001	0.0003 ± 0.001
Carbon dioxide	0.0030 ± 0.0005	0.002 ± 0.0005
Other volatile carbonaceous material; e.g., UDMH, MMH, alcohol	<0.2 0.12 ± 0.05	<0.1 0.11 ± 0.05

The helium used for specimen MJS-W-He-1 met the requirements of MIL-P-27407 with less than one part per million of hydrocarbons and a dew point of −84°C (−120°F) (cf. Section V-A).

III. Procedures

A. Test Specimen Preparation

All tests were made on uniaxially loaded fracture mechanics specimens containing part-through cracks (PTC). Specimens were configured and tested within the guidelines of ASTM Task Group E-24.01.05 for the PTC specimen (Ref. 7). General specimen geometry for all three types or specimens is shown in Fig. 5.

An electrical discharge machined (EDM) notch was used to start the crack. The location of the EDM notch for weld and HAZ specimens was determined by etching the edge of each specimen with Kroll's etch.

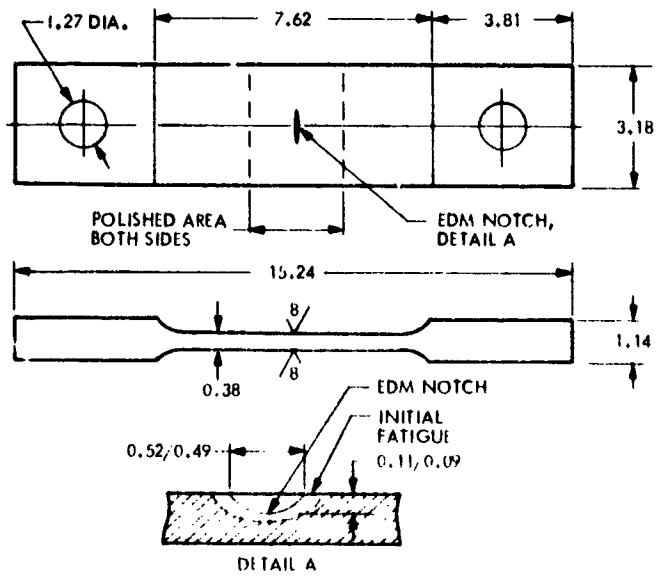

Fig. 5. Basic test specimen configuration

REPRODUCIBILITY OF THE ORIGINAL PAGE IS POOR

Precracking before sustained load testing was done by cyclically loading the EDM notch in bending. A maximum outer fiber cyclic stress of 482.6 MPa (70 ksi) was used to initiate the precrack at the root of the EDM notch, and a maximum outer fiber stress of 275.8 MPa (40 ksi) was used to extend the precrack to the initial dimensions of the sustained load test. A maximum-to-minimum stress ratio of 0.1 was used for all cyclic loading.

After precracking, all specimens were cleaned to the requirements for monopropellant propulsion systems (Ref. 8).

B. Sustained Load Testing

Sustained loading equipment and procedures were essentially the same as those used by Masters and Tiffany, from whom the testing techniques were learned (Ref. 9). Three specimens were loaded in tandem in a standard creep testing machine. The applied stress intensity during sustained loading was varied by changing the width of the three simultaneously loaded specimens. The test fluid was pressured into the crack tip using cups sealed with polytetrafluoroethylene O-ring seals. A matching cup and O-ring was used on the back face of the specimen so that the uniaxial stress field in the specimen was unperturbed. These procedures are described in detail in Ref. 10.

C. Crack Growth Determination

After sustained load testing, the cracks were "marked" by cyclic loading in air. Each specimen was then fractured in air with a monotonically increasing load at 21 to 24°C (70 to 75°F) to measure its fracture toughness, K_{IE}. A loading rate of approximately 18.5 MPa/s was used for these tests to simulate the rate of loading in a pressure vessel proof test.

The fracture surfaces were examined in a Cambridge Stereoscan scanning electron microscope (SEM) to measure any crack growth which occurred during the sustained load tests. Because the precrack and the mark which were made by cyclic loading are so different in fracture features from sustained load crack growth, as little as 0.0002 cm of growth can be accurately determined. For a 24-h test, this computes to be a crack growth rate as small as 2×10^{-11} m/s. Figure 6 is a graphic example of the sensitivity of this technique.

D. Stress Intensity Solution

The basic stress intensity used for the PTC specimens was the familiar Griffith–Irwin relationship as modified by Masters (Ref. 11):

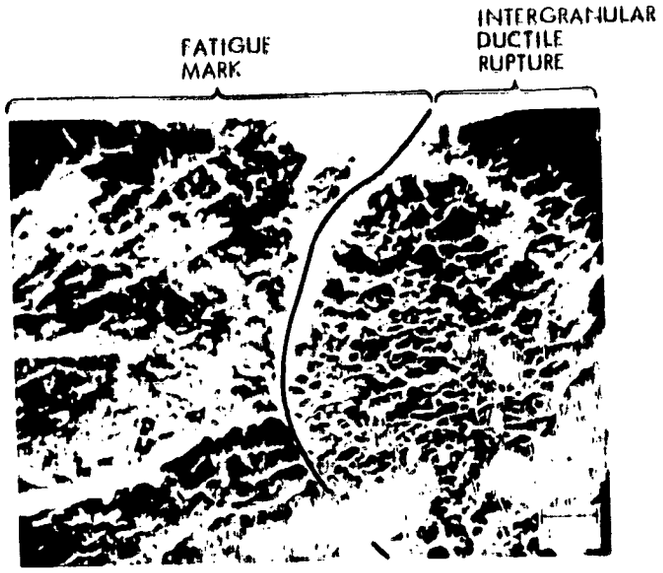

Fig. 6. SEM photomicrograph of boundary between fatigue "mark" and intergranular ductile rupture zone showing capability of growth measurement method (MJS-W-1)

$$K_I = \sqrt{1.21\pi(a/Q)}M_K\sigma \qquad (1)$$

where

K_I = stress intensity at the tip of a PTC
a = crack depth or minor semi-axis of a PTC
Q = Irwin's flaw shape parameter
M_K = Master's magnification factor
σ = remote gross uniaxial tensile stress

The subscript i denotes the initial condition at the start of the sustained load test, while the subscript E denotes the critical experimental fracture toughness at 21 to 24°C for the particular PTC specimen being tested.

E. Propellant Analyses

Samples of the propellants were transferred glass capsules without exposure to air. The capsule was placed in a stainless steel fixture and the propellant frozen by immersion in liquid nitrogen. The capsule tip was then broken and the volume of noncondensible gases measured in a calibrated vacuum system. The hydrazine was thawed and refrozen at −30°C (−22°F). All materials still in the gaseous state at that temperature [mainly ammonia (NH_3)] were measured. The purity of the resi-

dual hydrazine was determined by gas chromatography, which measures NH_3, H_2O, UDMH, and MMH. Aniline was determined colorimetrically. Metal content was analyzed by atomic absorption techniques. A turbidimetric method was used for low concentrations of chloride.

IV. Results

A. Sustained Load Crack Growth Data

Sustained load crack growth data for all the specimens are reported in Table 7. SEM photomicrographs of selected typical specimens are shown in Figs. 7 through 13.

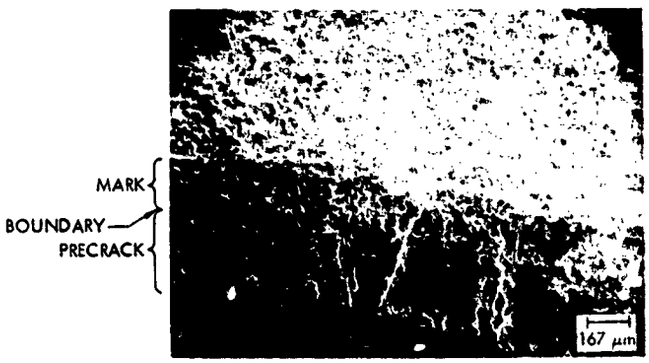

Fig. 7. SEM photomicrograph of precrack and fatigue "mark" typical of forging specimens exhibiting no SLCG (LCF-21)

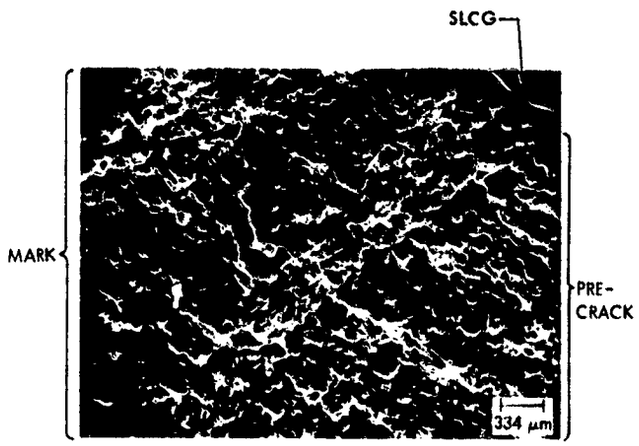

Fig. 8. SEM photomicrograph showing 0.0152 cm of growth by tra isgranular ductile rupture of aged forging after 24 h at 97% of K_{IE} (LCF-23)

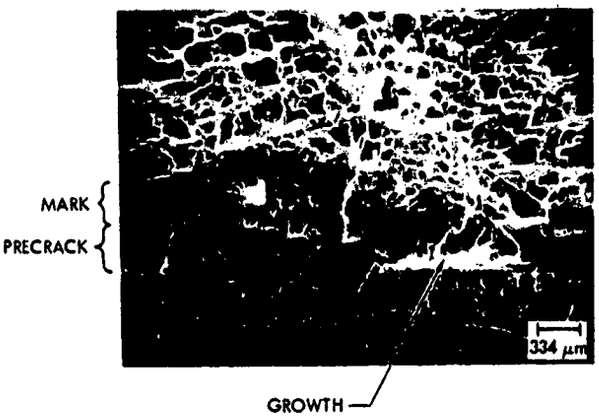

Fig. 9. SEM photomicrograph showing SLCG by intergranular ductile rupture of unaged weld in MIL-Spec hydrazine at 40–44°C at 50% of K_{IE} for 24 h (LCW-12)

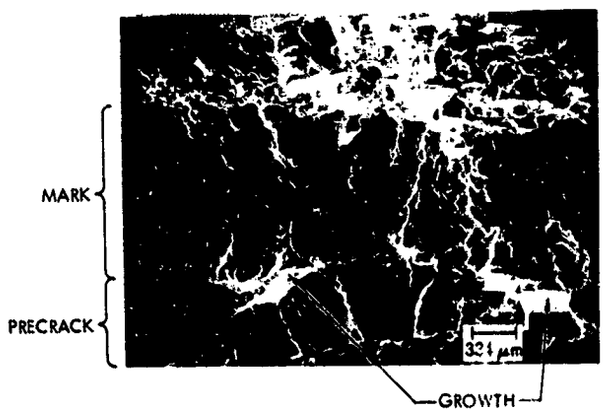

Fig. 10. SEM photomicrograph showing SLCG by intergranular ductile rupture of unaged weld in MIL-Spec hydrazine at 40–44°C at 63% of K_{IE} for 24 h (LCW-11)

Fig. 11. SEM photomicrograph of precrack and "mark" typical of HAZ specimens exhibiting no SLCG (LCH-3)

REPRODUCIBILITY OF THE
ORIGINAL PAGE IS POOR

Table 7. SLCG data for Ti-6Al-4V forgings, welds, and HAZ in various propellants at various temperatures

Specimen ID		Width, cm	Thickness, cm	Stress, MPa	Initial crack depth a_i, cm	Initial crack length $2C_i$, cm	Final crack depth a_f, cm	Growth $a_f - a_i$, cm	$\frac{\sigma}{\sigma_{ys}}$	Q_i	M_{Ki}	K_{Ii}, $MPa\sqrt{m}$	$\frac{K_{Ii}}{K_{IE}}$	Material	Environment	Temperature, °C	Duration of test, h
LCF	- 2	2.962	0.403	719.41	0.132	0.610	0.132	0	0.65	1.28	1.05	47.3	0.78	Forging (aged)	MIL-Spec hydrazine	40-44	24
	- 7	2.774	0.400	774.99	0.145	0.612	0.145	0	0.70	1.31	1.05	52.8	0.80				
	-23	2.492	0.400	856.78	0.160	0.655	0.175	0.0152	0.78	1.32	1.07	62.3	0.97				
	-30	2.679	0.400	800.74	0.157	0.630	0.157	0	0.73	1.34	1.06	56.7	0.91				
LCW	- 2	3.218	0.408	570.09	0.170	0.589	0.183	0.0127	0.64	1.50	1.06	39.7	0.71	Weld (unaged)			
	- 3	3.383	0.399	555.05	0.175	0.597	0.183	0.0076	0.62	1.52	1.06	38.9	0.69				
	-10	3.051	0.403	461.22	0.188	0.622	0.188	0.0120	0.52	1.57	1.07	33.3	0.65				
	-11	3.152	0.403	446.36	0.157	0.582	0.163	0.0051	0.50	1.48	1.05	29.8	0.63				
	-12	3.256	0.403	432.35	0.168	0.566	0.170	0.0025	0.48	1.55	1.06	29.3	0.50				
	-25	3.175	0.284	579.16	0.142	0.673	0.147	0.0051	0.65	1.26	1.13	42.9	0.65				
LCH	- 1	2.278	0.400	762.79	0.175	0.536	0.178	0.0025	0.79	1.55	1.05	52.5	0.70	HAZ (unaged)			
	- 2	2.410	0.402	717.36	0.178	0.589	0.185	0.0076	0.74	1.51	1.06	50.9	0.75				
	- 3	2.537	0.404	678.03	0.180	0.602	0.180	0	0.70	1.51	1.07	48.9	0.78				
	-10	2.421	0.404	791.50	0.168	0.602	0.173	0.0051	0.82	1.41	1.06	56.4	0.85				
	-11	2.482	0.402	774.99	0.173	0.638	0.180	0.0076	0.80	1.39	1.07	57.0	—				
	-12	2.545	0.403	754.22	0.183	0.632	0.185	0.0025	0.78	1.46	1.07	55.7	0.75				
LCF	- 3	2.959	0.397	683.02	0.145	0.612	0.145	0	0.62	1.34	1.05	45.9	0.75	Forging (aged)		60-63	
	- 8	2.771	0.398	727.95	0.142	0.602	0.142	0	0.66	1.34	1.05	48.6	0.77				
	-14	3.178	0.399	633.64	0.122	0.571	0.122	0	0.57	1.30	1.04	39.8	0.62				
	-18	2.550	0.394	798.75	0.163	0.627	0.168	0.0051	0.72	1.35	1.07	57.8	0.91				
	-22	2.494	0.403	798.12	0.132	0.587	0.135	0.0025	0.72	1.28	1.04	52.5	0.89				
	-29	2.680	0.396	755.75	0.170	0.653	0.175	0.0051	0.69	1.46	1.07	53.8	0.86				
LCW	- 4	3.048	0.407	599.68	0.168	0.571	0.244	0.0762	0.67	1.51	1.05	40.9	0.68	Weld (unaged)			
	- 5	3.213	0.405	571.73	0.168	0.541	0.185	0.0178	0.64	1.57	1.05	38.2	0.70				
	- 6	3.383	0.403	545.02	0.165	0.571	0.175	0.0102	0.61	1.51	1.06	37.3	0.69				
	-13	3.051	0.399	451.67	0.173	0.564	0.175	0.0025	0.50	1.58	1.06	30.9	0.56				
	-14	3.147	0.409	426.94	0.183	0.612	0.185	0.0025	0.48	1.57	1.06	30.1	0.57				
	-15	3.254	0.398	425.08	0.163	0.584	0.163	0.0050	0.48	1.51	1.06	28.9	0.64				

Table 7 (contd)

Specimen ID		Width, cm	Thickness, cm	Stress, MPa	Initial crack depth a_i, cm	Initial crack length $2C_i$, cm	Final crack depth a_f, cm	Growth $a_f - a_i$, cm	$\frac{\sigma}{\sigma_{ys}}$	Q_i	M_{Ki}	K_{Ii}, $MPa\sqrt{m}$	$\frac{K_{Ii}}{K_{IE}}$	Material	Environment	Temperature, °C	Duration of test, h
LCH	- 4	2.273	0.408	808.76	0.183	0.620	0.190	[a]	0.84	1.45	1.07	59.9	0.90	HAZ (unaged)	MIL-Spec hydrazine	60-63	24
	- 5	2.418	0.404	766.55	0.170	0.617	0.175	0.0051	0.79	1.42	1.06	54.8	0.77				
	- 6	2.548	0.398	739.	0.173	0.620	0.180	0.0076	0.77	1.43	1.07	53.6	0.79				
	-13	2.418	0.404	818.04	0.173	0.615	0.188	0.0152	0.85	1.41	1.06	59.1	0.87				
	-14	2.479	0.402	800.95	0.165	0.589	0.173	0.0076	0.83	1.41	1.06	56.7	0.81				
	-15	2.550	0.404	775.67	0.168	0.587	0.175	0.0076	0.80	1.43	1.06	54.8	0.78				
LCF	- 4	2.974	0.398	641.77	0.135	0.602	0.135	0	0.58	1.32	1.05	42.0	0.63	Forging (aged)		71-74	
	- 9	2.786	0.397	686.38	0.142	0.610	0.140	0	0.62	1.33	1.05	45.9	0.74				
	-15	3.183	0.397	600.92	0.137	0.602	0.137	0	0.55	1.34	1.04	39.0	0.63				
	-17	3.071	0.396	732.07	0.160	0.630	0.160	0	0.66	1.38	1.06	51.5	0.79				
	-21	2.967	0.403	743.93	0.130	0.589	0.130	0	0.67	1.29	1.04	47.8	0.78				
	-28	3.178	0.398	703.88	0.150	0.630	0.150	0	0.64	1.34	1.06	48.7	0.80				
LCW	- 7	3.051	0.404	581.31	0.170	0.599	0.180	0.0102	0.65	1.48	1.06	40.8	0.77	Weld (unaged)			
	- 8	3.216	0.409	544.27	0.180	0.615	0.193	0.0127	0.61	1.52	1.06	38.7	0.73				
	- 9	3.386	0.408	517.56	0.175	0.589	0.193	0.0178	0.56	1.55	1.06	35.9	0.63				
	-16	3.048	0.400	582.96	0.165	0.574	0.170	0.0051	0.65	1.50	1.06	40.0	0.87				
	-17	3.147	0.409	555.30	0.168	0.577	0.173	0.0051	0.62	1.51	1.05	37.6	0.72				
	-18	3.251	0.409	534.64	0.170	0.594	0.173	0.0025	0.60	1.51	1.06	37.0	0.73				
LCH	- 7	2.296	0.402	760.53	0.168	0.625	0.175	0.0076	0.79	1.39	1.07	55.1	0.81	HAZ (unaged)			
	- 8	2.423	0.406	713.46	0.170	0.607	0.173	0.0025	0.74	1.44	1.06	50.7	0.74				
	- 9	2.540	0.398	694.54	0.170	0.610	0.170	0	0.72	1.44	1.06	49.3	0.71				
	-16	2.418	0.404	727.89	0.183	0.645	0.190	0.0076	0.75	1.45	1.07	54.0	0.76				
	-17	2.482	0.405	707.04	0.173	0.602	0.175	0.0025	0.73	1.46	1.06	50.2	0.68				
	-18	2.545	0.405	688.53	0.168	0.559	0.168	0	0.71	1.51	1.05	47.0	69				
LCW	-19	3.045	0.399	717.15	0.173	0.645	0.185	0.0127	0.80	1.38	1.07	52.9	0.81	Weld (aged)		40-44	
	-21	3.373	0.401	643.39	0.165	0.630	0.218	0.0533	0.72	1.39	1.06	45.8	0.90				
	-23	3.147	0.406	496.52	0.241	0.777	0.241	0	0.55	1.60	1.12	42.0	0.91				
	-24	3.254	0.406	480.84	0.168	0.592	0.168	0	0.54	1.51	1.06	33.1	—				
	-19A	2.545	0.282	620.03	0.135	0.579	0.135	0	0.69	1.32	1.11	42.9	0.68				
	-20A	2.865	0.280	555.27	0.132	0.592	0.132	0	0.62	1.31	1.11	38.1	0.67				
	-21A	3.178	0.284	493.07	0.140	0.587	0.140	0	0.55	1.36	1.11	34.2	0.65				

Table 7 (contd)

Specimen ID	Width, cm	Thickness, cm	Stress, MPa	Initial crack depth a_i, cm	Initial crack length $2C_i$, cm	Final crack depth a_f, cm	Growth $a_f - a_i$, cm	$\frac{\sigma}{\sigma_{ys}}$	Q_i	M_{Ki}	K_{Ii}, $MPa\sqrt{m}$	$\frac{K_{Ii}}{K_{IE}}$	Material	Environment	Temperature, °C	Duration of test, h
LCH -19	2.299	0.405	813.02	0.165	0.607	0.165	0	0.84	1.37	1.06	58.4	0.87	HAZ (aged)	MIL-Spec hydrazine	40-44	24
-20	2.423	0.403	774.67	0.165	0.582	0.165	0	0.80	1.43	1.06	54.4	0.85				
-21	2.545	0.401	741.77	0.175	0.577	0.175	0	0.77	1.53	1.06	51.9	0.75				
-22	2.299	0.404	814.05	0.173	0.582	0.173	0	0.84	1.45	1.06	58.1	—				
MJS-W - 1	3.038	0.401	590.17	0.178	0.544	0.178	[a]	0.66	1.64	1.05	39.8	0.72	Weld (unaged)	Refined hydrazine		
- 4	3.051	0.403	603.19	0.163	0.569	0.165	0.0025	0.67	1.49	1.05	40.8	0.67				
- 5	3.150	0.402	586.06	0.170	0.564	0.173	0.0025	0.65	1.54	1.05	39.9	0.72				
- 6	3.254	0.404	564.81	0.170	0.549	0.201	0.0310	0.63	1.56	1.05	38.1	0.78				
MJS-H - 1	2.537	0.402	695.40	0.173	0.582	0.173	0	0.63	1.53	1.06	48.4	0.69	HAZ (unaged)			
- 2	2.408	0.400	736.54	0.180	0.549	0.180	0	0.67	1.64	1.05	50.0	0.69				
- 3	2.286	0.407	762.73	0.165	0.559	0.165	0	0.69	1.52	1.05	51.4	0.69				
- 4	2.540	0.407	780.39	0.165	0.571	0.168	0.0025	0.81	1.44	1.05	54.1	0.77				
- 5	2.484	0.407	799.44	0.185	0.632	0.188	0.0025	0.83	1.45	1.07	59.7	0.78				
- 6	2.421	0.405	824.53	0.173	0.599	0.183	0.0102	0.85	1.43	1.06	59.2	0.86				
LCF -13	2.964	0.402	728.82	0.165	0.665	0.165	0	0.66	1.36	1.07	53.0	0.89	Forging (aged)			
-19	2.774	0.394	795.44	0.155	0.627	0.157	0.0025	0.72	1.33	1.06	56.2	0.89				
-24	3.180	0.402	679.76	0.147	0.643	0.147	0	0.62	1.29	1.06	47.5	0.83				
-25	2.685	0.401	757.64	0.155	0.658	0.157	0.0025	0.69	1.33	1.06	53.4	—				
-26	2.583	0.401	787.94	0.152	0.655	0.160	0.0076	0.71	1.30	1.06	55.7	0.94				
-27	2.499	0.403	810.76	0.157	0.655	0.168	0.0102	0.74	1.32	1.06	57.9	0.95				
MJS-W-He - 1	3.180	0.285	648.11	0.137	0.671	0.140	0.0025	0.81	1.45	1.13	52.2	0.86	Weld (unaged)	Helium	21-24	24

[a]Growth to side only.

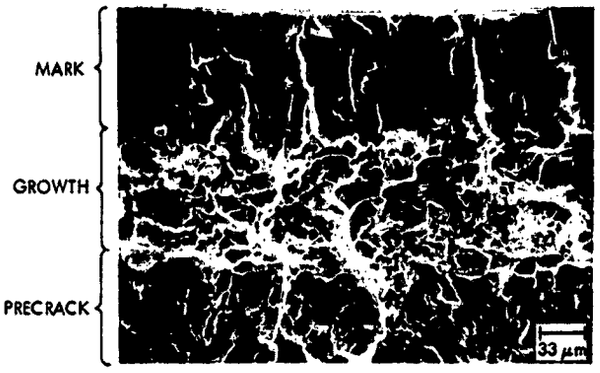

Fig. 12. SEM photomicrograph showing SLCG by transgranular ductile rupture typical of unaged HAZ in hydrazine (MJS-H-6)

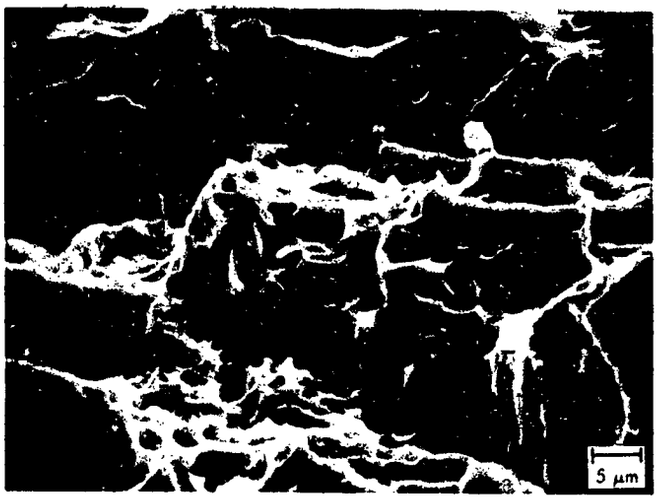

Fig. 13. SEM photomicrograph of growth by transgranular ductile rupture of unaged weld in helium at 21–24°C at 86% of K_{IE} for 24 h (MJS-W-He-1)

The STA forging material was found to be unaffected by either propellant. The center of the unaged weld metal was found to be the most susceptible to SLCG in both propellants. The susceptibility of the unaged HAZ was intermediate between the STA forging and the unaged weld. Aging the weld and HAZ after welding completely eliminated the susceptibility of the weld and HAZ to SLCG due to hydrazine. Both the unaged weld and unaged HAZ were more susceptible to SLCG in MIL-Spec hydrazine than in refined hydrazine.

The microstructure of this alloy can be simply described as transformed alpha-beta platelets within prior beta grain boundaries. The forged material also has a primary alpha phase which does not exist in the weld. The prior beta grains are very small in the forging and cannot usually be seen (Fig. 1). However, in the weld, the prior beta grains are as long as the weld is thick, and the alpha-beta platelets form a network of low-angle subgrains (Figs. 4, 14).

All crack growth observed in aged forging specimens was transgranular ductile rupture like that seen in Fig. 8. All crack growth in unaged HAZ was transgranular ductile rupture typified by Fig. 12. No growth was seen in aged HAZ.

Both aged and unaged welds showed two types of growth: intergranular ductile rupture along the low-angle subgrain boundaries (Figs. 14 through 17) and transgranular ductile rupture at approximately 45 deg to the low-angle subgrain boundaries (Fig. 18).

No particular trend in weld fracture mode could be seen with respect to SLCG, rapid fracture in air (K_{IE} tests), or propellant chemistry. Both types of fracture were found in SLCG in both propellants. Both types of fracture were also found in rapid fracture in air. Fast fracture in air could not be determined fractographically from SLCG in hydrazine (compare Figs. 16 and 17). The only apparent difference between SLCG in hydrazine and rapid fracture in air was the stress intensity at which each occurred. SLCG in helium was entirely transgranular ductile rupture (Fig. 13).

When extensive SLCG occurred, the greatest amount of growth was to the side rather than at the center of the crack, where the stress intensity is greatest (Fig. 19).

Fig. 14. Photomicrograph showing SLCG along low-angle subgrain boundaries of unaged weld (MJS-W-1; Kroll's etch)

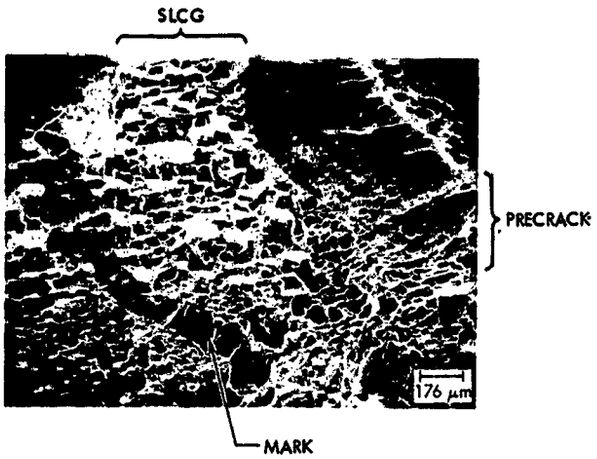

Fig. 15. SEM photomicrograph showing SLCG by intergranular ductile rupture along low-angle subgrain boundaries of unaged weld in refined hydrazine at 40–44°C at 72% of K_{IE} for 24 h (MJS-W-1)

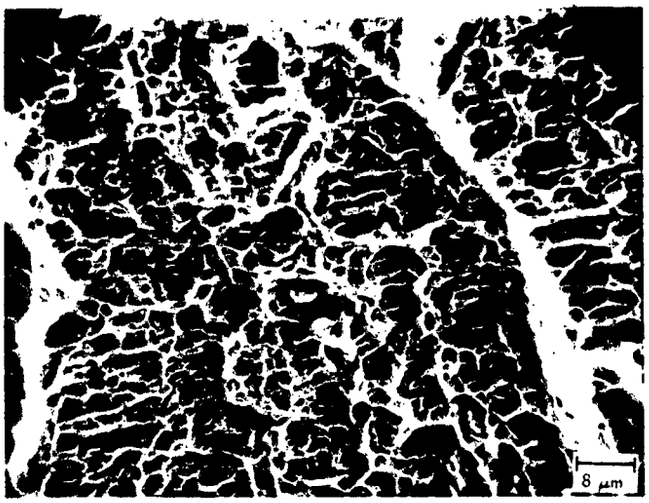

Fig. 17. SEM photomicrograph of rapid fracture in air by intergranular ductile rupture along low-angle subgrain boundaries of unaged weld (MJS-W-1)

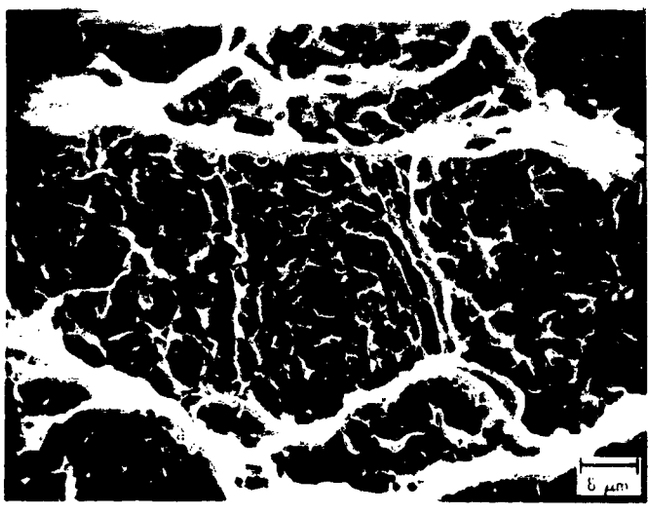

Fig. 16. SEM photomicrograph of SLCG by intergranular ductile rupture along low-angle subgrain boundaries of unaged weld in refined hydrazine at 40–44°C at 72% of K_{IE} for 24 h (MJS-W-1)

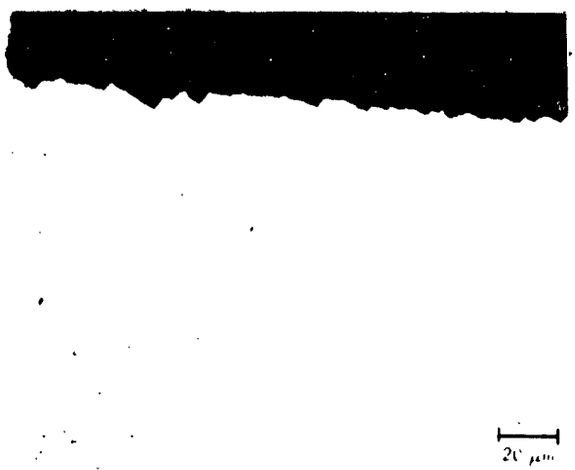

Fig. 18. Photomicrograph showing transgranular fracture across low-angle subgrains (MJS-W-1; Kroll's etch)

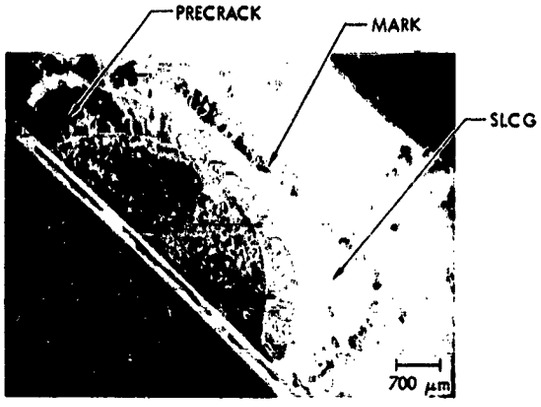

Fig. 19. SEM photomicrograph showing more SLCG to the side than at the center of the crack (MJS-W-6)

Also, specimens LCW-15 and MJS-W-1 show growth only to the side (Table 7). Masters has suggested that this phenomenon is due to a lower fracture toughness of the material in this direction (Ref. 11).

B. Fracture Toughness Data

The experimental fracture toughness K_{IE} at 21 to 24°C of each of the SLCG specimens is reported in Table 8. Data for specimens LCF-25, LCW-24, LCH-11, and LCH-22 are not included, either because the final flaw was too deep for full elastic constraint at the tip of the PTC or because the specimen broke during marking.

V. Discussion

A. Role of Hydrazine in SLCG of Unaged Welds

Because the fracture mode for SLCG of the unaged weld in hydrazine and the fracture mode for rapid fracture in air were indistinguishable fractographically, a question arose concerning the susceptibility of the unaged weld to SLCG in helium commonly used to pressurize hydrazine tanks. Therefore specimen MJS-W-He-1 was tested in helium at 21 to 24°C at 86% of K_{IE} for 24 h. Only 0.0025 cm of growth occurred at this level in helium, thereby showing that the SLCG in the unaged weld seen in hydrazine at much lower applied stress intensities was actually caused by the hydrazine. Also, some concern arose that the high susceptibility of the unaged weld to SLCG in hydrazine might be unique to the MJS'77 spacecraft propellant tank weld joint configuration, so specimen LCW-25 from an unaged weld panel of the VO'75 spacecraft propellant tank weld joint configuration was tested. This specimen showed identical SLCG in hydrazine to that seen in the other specimen (Table 7).

B Design Curves

Reference 1 describes in detail the application of fracture mechanics data to pressure vessel design. Therefore, only the design curves seen in Figs. 20 through 25 will be presented here. The authors chose to plot the

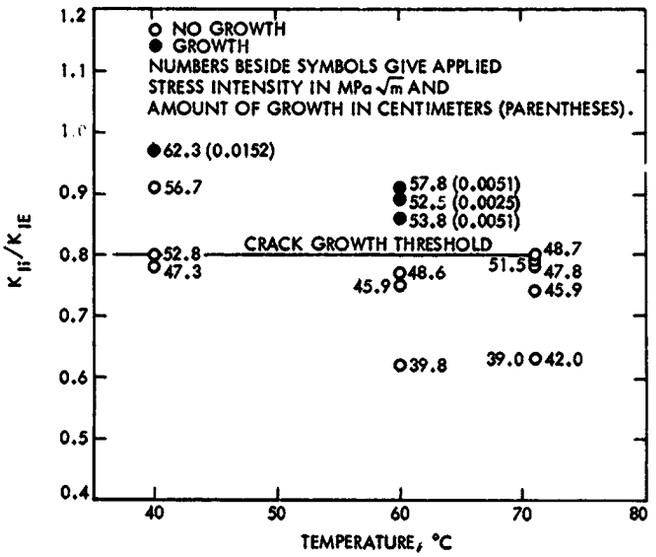

Fig. 20. Temperature versus SLCG threshold for 24-h exposure of aged Ti-6Al-4V forgings in MIL-Spec hydrazine

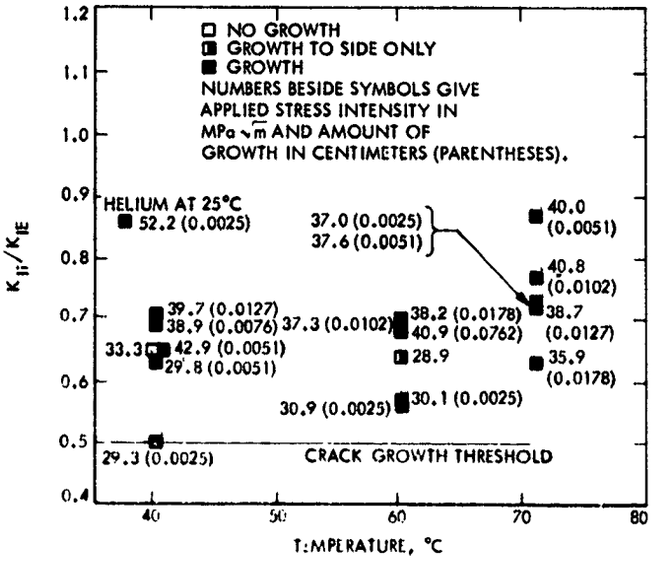

Fig. 21. Temperature versus SLCG threshold for 24-h exposure of unaged Ti-6Al-4V welds in MIL-Spec hydrazine

REPRODUCIBILITY OF THE
ORIGINAL PAGE IS POOR

Table 8. Experimental fracture toughness (K_{IE}) data for Ti-6Al-4V forgings, welds, and HAZ

Specimen ID		Width, cm	Thickness, cm	Failure stress, MPa	Crack depth a, cm	Crack length $2c$, cm	$\frac{\sigma}{\sigma_{ys}}$	Q	M_K	K_{IE}, MPa$\sqrt{m}$	Material	Temperature, °C
LCF	- 2	2.962	0.403	865.8	0.145	0.655	0.79	1.25	1.06	60.9	Forging (aged)	21-24
	- 3	2.959	0.397	860.9	0.152	0.627	0.78	1.31	1.06	61.0		
	- 4	2.974	0.398	924.3	0.150	0.648	0.84	1.25	1.06	66.2		
	- 7	2.774	0.400	932.6	0.150	0.632	0.85	1.27	1.06	66.3		
	- 8	2.771	0.398	897.3	0.150	0.630	0.81	1.28	1.06	63.4		
	- 9	2.786	0.397	880.1	0.150	0.635	0.80	1.29	1.06	62.0		
	-13	2.964	0.402	763.1	0.168	0.818	0.69	1.25	1.09	59.5		
	-14	3.178	0.399	956.6	0.130	0.577	0.87	1.24	1.05	63.3		
	-15	3.183	0.397	883.1	0.147	0.630	0.80	1.28	1.06	62.0		
	-17	3.071	0.396	880.3	0.170	0.671	0.80	1.34	1.07	65.5		
	-18	2.550	0.394	823.5	0.168	0.757	0.75	1.26	1.09	63.8		
	-19	2.774	0.394	809.9	0.163	0.798	0.73	1.22	1.09	62.9		
	-21	2.967	0.403	892.7	0.145	0.617	0.81	1.28	1.05	61.4		
	-22	2.494	0.403	822.9	0.142	0.729	0.75	1.19	1.06	58.8		
	-23	2.492	0.400	812.2	0.178	0.785	0.74	1.28	1.09	64.3		
	-24	3.180	0.402	752.3	0.157	0.798	0.68	1.22	1.08	56.9		
	-26	2.583	0.401	719.6	0.218	0.739	0.65	1.52	1.11	59.0		
	-27	2.499	0.403	710.6	0.249	0.765	0.64	1.63	1.12	60.7		
	-28	3.178	0.398	848.2	0.157	0.668	0.77	1.29	1.05	60.7		
	-29	2.680	0.396	804.3	0.175	0.742	0.73	1.31	1.09	62.5		
	-30	2.670	0.400	838.3	0.157	0.726	0.76	1.23	1.07	62.6		
LCW	- 2	3.218	0.408	742.3	0.203	0.630	0.83	1.55	1.07	56.0	Weld (unaged)	
	- 3	3.383	0.399	741.2	0.201	0.638	0.83	1.53	1.08	56.5		
	- 4	3.048	0.407	693.9	0.251	0.759	0.77	1.61	1.12	59.9		
	- 5	3.213	0.405	692.2	0.190	0.729	0.77	1.37	1.09	54.8		
	- 6	3.383	0.403	695.9	0.206	0.645	0.78	1.56	1.09	53.7		
	- 7	3.051	0.404	681.4	0.211	0.663	0.76	1.56	1.08	52.8		
	- 8	3.216	0.409	680.6	0.211	0.671	0.76	1.55	1.08	52.9		
	- 9	3.386	0.408	734.0	0.206	0.650	0.82	1.53	1.08	56.7		
	-10	3.051	0.403	683.2	0.193	0.640	0.76	1.51	1.07	51.0		
	-11	3.152	0.403	629.6	0.188	0.658	0.70	1.47	1.08	47.4		
	-12	3.256	0.403	808.1	0.180	0.589	0.90	1.45	1.06	58.9		
	-13	3.051	0.399	704.9	0.188	0.714	0.79	1.38	1.09	55.3		
	-14	3.147	0.409	687.9	0.201	0.665	0.77	1.51	1.08	52.9		
	-15	3.251	0.398	628.7	0.170	0.627	0.70	1.43	1.07	45.3		
	-16	3.048	0.400	626.0	0.188	0.627	0.70	1.53	1.07	45.8		
	-17	3.147	0.409	703.0	0.196	0.627	0.79	1.54	1.07	52.3		
	-18	3.251	0.409	676.6	0.203	0.640	0.76	1.56	1.07	50.9		
	-19	3.045	0.399	753.4	0.216	0.795	0.84	1.38	1.12	65.1	Weld (aged)	
	-21	3.373	0.401	618.7	0.274	0.716	0.69	1.85	1.10	51.1		

Table 8 (contd)

Specimen ID	Width, cm	Thickness, cm	Failure stress, MPa	Crack depth a, cm	Crack length $2c$, cm	$\frac{\sigma}{\sigma_{ys}}$	Q	M_K	K_{IE}, MPa$\sqrt{m}$	Material	Temperature, °C
LCW -23	3.147	0.406	541.0	0.241	0.777	0.60	1.58	1.12	46.2	Weld	21-24
(contd) -25	3.175	0.284	835.7	0.150	0.673	0.93	1.20	1.14	65.6	(aged)	
-19A	2.545	0.282	855.5	0.142	0.589	0.96	1.24	1.12	63.3	↓	
-20A	2.865	0.280	744.2	0.152	0.627	0.83	1.29	1.14	56.6		
-21A	3.178	0.284	705.8	0.155	0.605	0.79	1.35	1.13	52.8		
LCH - 1	2.278	0.400	943.0	0.211	0.592	0.98	1.62	1.06	74.8	HAZ	
- 2	2.410	0.402	897.2	0.203	0.617	0.93	1.54	1.07	68.0	(unaged)	
- 3	2.537	0.404	830.8	0.216	0.627	0.86	1.63	1.07	63.1		
- 4	2.273	0.408	785.5	0.257	0.732	0.81	1.66	1.10	66.3		
- 5	2.418	0.404	882.6	0.211	0.678	0.91	1.48	1.09	70.8		
- 6	2.548	0.398	799.3	0.246	0.726	0.83	1.62	1.11	67.5		
- 7	2.296	0.402	900.0	0.188	0.640	0.93	1.42	1.07	68.2		
- 8	2.423	0.406	906.2	0.190	0.635	0.94	1.44	1.07	68.8		
- 9	2.540	0.398	870.3	0.208	0.676	0.90	1.47	1.08	69.0		
-10	2.421	0.404	816.8	0.229	0.696	0.85	1.57	1.09	66.3		
-12	2.545	0.403	956.9	0.198	0.643	0.99	1.45	1.08	74.5		
-13	2.418	0.404	871.0	0.208	0.653	0.90	1.51	1.08	68.1		
-14	2.479	0.402	938.0	0.180	0.605	0.97	1.42	1.07	69.8		
-15	2.550	0.404	913.2	0.218	0.635	0.95	1.60	1.07	70.3		
-16	2.418	0.404	892.4	0.216	0.668	0.92	1.52	1.08	70.8		
-17	2.482	0.405	980.4	0.183	0.615	1.00	1.40	1.07	74.0		
-18	2.545	0.405	901.3	0.201	0.615	0.93	1.53	1.07	68.1	↓	
-19	2.299	0.405	802.0	0.254	0.711	0.83	1.67	1.10	67.0	HAZ	
-20	2.423	0.403	827.7	0.244	0.645	0.86	1.77	1.07	64.1	(aged)	
-21	2.545	0.401	925.0	0.190	0.610	0.96	1.48	1.07	69.2	↓	
MJS-W - 1	3.038	0.401	721.0	0.190	0.653	0.81	1.45	1.08	55.1	Weld	
- 4	3.051	0.403	816.7	0.183	0.612	0.91	1.44	1.07	60.7	(unaged)	
- 5	3.150	0.402	746.1	0.183	0.612	0.83	1.46	1.07	55.1		
- 6	3.254	0.404	631.7	0.241	0.653	0.71	1.75	1.07	48.9	↓	
MJS-H - 1	2.537	0.402	902.2	0.173	0.734	0.82	1.27	1.08	70.0	HAZ	
- 2	2.408	0.400	914.2	0.180	0.737	0.83	1.30	1.09	72.4	(unaged)	
- 3	2.286	0.407	989.5	0.165	0.711	0.90	1.25	1.07	75.1		
- 4	2.540	0.407	956.6	0.188	0.599	0.99	1.47	1.06	70.7		
- 5	2.484	0.407	989.9	0.196	0.640	1.00	1.43	1.07	76.4		
- 6	2.421	0.405	908.8	0.198	0.627	0.94	1.49	1.07	69.1	↓	↓
MJS-W-He - 1	3.180	0.285	723.9	0.211	0.724	0.81	1.45	1.13	60.8	Weld (unaged)	

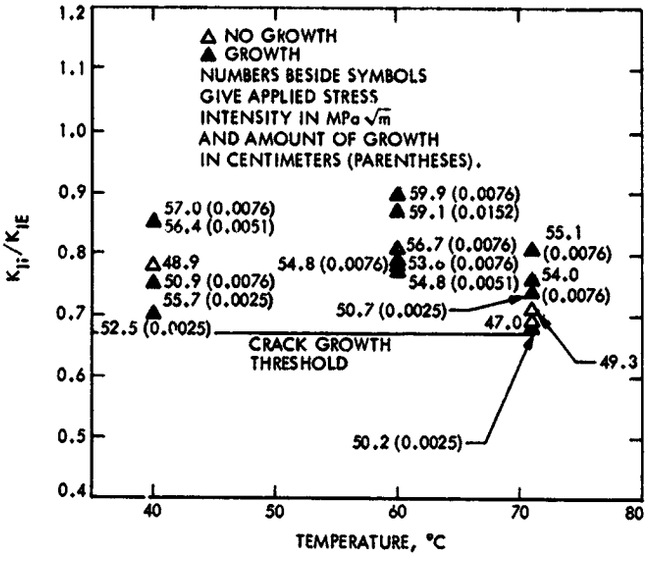

Fig. 22. Temperature versus SLCG threshold for 24-h exposure of unaged Ti-6Al-4V HAZ in MIL-Spec hydrazine

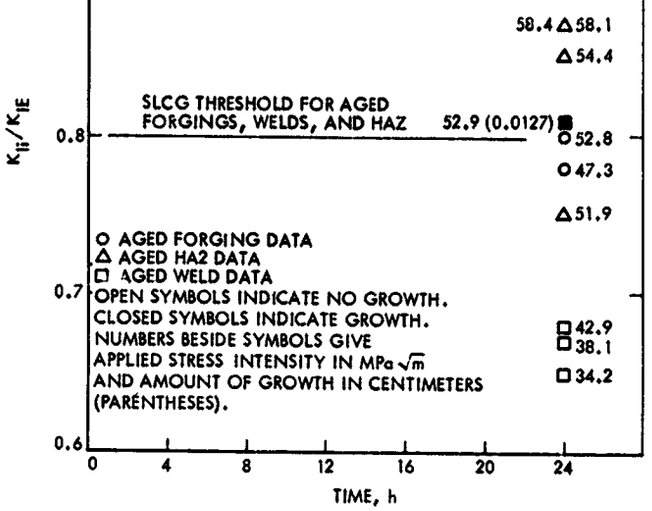

Fig. 24. SLCG threshold versus time for aged Ti-6Al-4V forgings, aged welds, and aged HAZ in MIL-Spec hydrazine at 40–44°C

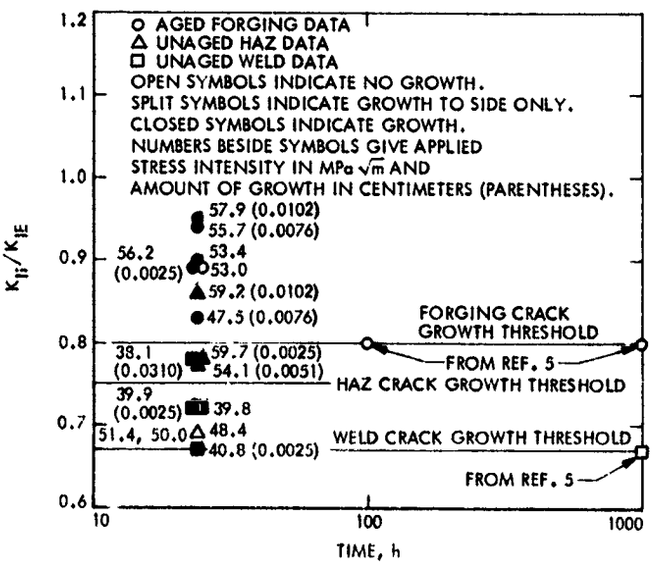

Fig. 23. SLCG threshold versus time for aged Ti-6Al-4V forgings, unaged welds, and unaged HAZ in refined hydrazine at 40–44°C

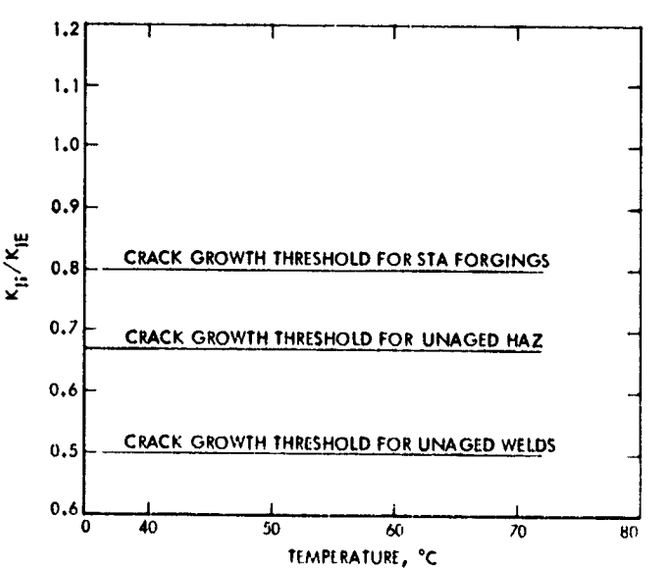

Fig. 25. Master design curve for "as welded" Ti-6Al-4V tanks in MIL-Spec hydrazine

REPRODUCIBILITY OF THE
ORIGINAL PAGE IS POOR

design curves as functions of the applied stress intensity ratio K_{Ii}/K_{IE}, because it is their opinion that this ratio is the true material property controlling SLCG for this alloy in these environments. The actual applied stress intensity K_{Ii} is recorded alongside each data point for the benefit of those whose design approach is based on this parameter only. The crack growth thresholds are recommended on the basis of the observed crack growth rates. No threshold above 80% of K_{IE} was recommended because of the SLCG observed in helium.

The apparent decrease in susceptibility to SLCG at the higher temperatures seen in Figs. 20 through 22 is believed to be caused by plotting the data for all temperatures as a function of the inverse of K_{IE} at 21 to 24°C. The actual K_{IE} at the higher sustained load test temperatures is higher than K_{IE} at 21 to 24°C. Therefore, the ratio of applied stress intensity at the sustained load test temperature to the fracture toughness at the sustained load test temperature, $K_{Ii}(71°C)/K_{IE}(71°C)$, is actually lower than the ratio that was plotted.

VI. Conclusions

(1) Extreme susceptibility to SLCG in hydrazine is a universal property of unaged weld metal in Ti-6Al-4V titanium alloy of normal interstitial content.

(2) Aging both weld metal and HAZ at 510°C for 4 h after welding completely removes all susceptibility to SLCG induced by hydrazine, as can be seen by comparing the 50% threshold of Fig. 21 to the 80% threshold of Fig. 24.

(3) It is not known whether the growth observed in the aged forgings, welds, and HAZ at stress intensities above 80% of K_{IE} was actually SLCG or subcritical growth on loading. The extremely low amounts of this growth such as seen in specimen LCF-23 suggests that the aged forging, welds, and HAZ may have a very sharp R-curve (Ref. 12).

(4) Unaged weld metal and unaged HAZ are less susceptible to SLCG in refined hydrazine than in MIL-Spec hydrazine (compare Figs. 21, 22, and 23).

(5) Aged forgings, aged and unaged welds, and aged and unaged HAZ made from aged forgings do not exhibit the SLCG behavior at low stress intensities in inert environments that was reported in Refs. 13, 14, and 15 for annealed Ti-6Al-4V plate in inert environments.

References

1. Tiffany, C. F., *Fracture Control of Metallic Pressure Vessels*, NASA SP-8040, National Aeronautics and Space Administration, Washington, D.C., May 1970.

2. *NASA Aerospace Pressure Vessel Safety Standard*, NASA NSS-HP1740.1, National Aeronautics and Space Administration, Washington, D.C., February 22, 1974.

3. *Functional Requirements, Mariner Jupiter/Saturn 1977 Structural Design Criteria*, Document MJS77-3-190, Jet Propulsion Laboratory, Pasadena, California, March 3, 1975 (JPL internal document).

4. King, J. P., and Johnson, K. R., *Space Shuttle Orbiter Fracture Control Plan*, Document SD-73-SH-0082 A, Rockwell International, Los Angeles, California, September 1974.

5. Bolstad, D. A., *Viking 75 Material Qualification Test Report of Fracture Mechanics Evaluation for the Viking Lander Pressure Vessels*, Report TR3720358, Martin Marietta Corporation, Denver, Colorado, February 1973.

6. Lewis, J. C., *General Fabrication Specification for Heat Treated Titanium Alloy (Ti-6Al-4V, STA) Pressure Vessels for Flight Equipment*, Specification FS509333, Jet Propulsion Laboratory, Pasadena, California, July 30, 1974 (JPL internal document).

7. Orange, T., "Fracture Testing with Surface Cracked Specimen," *Journal of Testing and Evaluation*, Vol. 3, No. 5, September 1975, pp. 335–342.

8. Lumsden, J. M., *Detail Specification for General Cleaning Requirements for Spacecraft Propulsion Systems and Support Equipment*, Specification FS504574, Revision C, Jet Propulsion Laboratory, Pasadena, California, May 28, 1974 (JPL internal document).

9. Masters, J. N., et al., *Fracture and Nitrogen Tetroxide/Sustained Load Flaw Growth of 6Al-4V Titanium*, Document 610-98, Jet Propulsion Laboratory, Pasadena, California, October 1969 (JPL internal document).

10. Toth, L. R. and Lewis, J. C., *Effect of Chloride Ion Content in Unsymmetrical Dimethylhydrazine Propellant on Fracture Properties of Structural Alloys*, AFRPL-TR-76-1, Air Force Rocket Propulsion Laboratory, Edwards Air Force Base, California, January 1976.

11. Masters, J. N., et al., *Investigation of Deep Flaws in Thin Walled Tanks*, NASA CR-72606, National Aeronautics and Space Administration, Washington, D.C., December 1969.

12. *Fracture Toughness Evaluation by R-Curve Methods*, ASTM Special Technical Publication 527, American Society for Testing and Materials, Philadelphia, Pennsylvania, April 1973.

13. Yoder, G. R., et al., "The Cracking of Ti-6Al-4V Alloys Under Sustained Load in Ambient Air," *Transactions of ASME, Series H, Journal of Engineering Materials and Technology*, Vol. 96, 1974, pp. 268–274.

14. Meyn, D. A., "Effect of Hydrogen on Fracture and Inert-Environment Sustained Load Cracking Resistance of α-β Titanium Alloys," *Metallurgical Transactions*, Vol. 5, 1974, pp. 2405–2414.

15. Williams, D. N., "Subcritical Crack Growth Under Sustained Load," ibid., pp. 2351–2358.

NASA JPL Comm LA Calif